



Published in final edited form as:

J Am Chem Soc. 2009 June 24; 131(24): 8425–8433. doi:10.1021/ja900781n.

Radical Reactions with Double Memory of Chirality (²MOC) for the Enantiospecific Synthesis of Adjacent Stereogenic Quaternary Centers in Solution: Cleavage and Bonding Faster than Radical Rotation

Marino J. E. Resendiz[†], Farnosh Family[†], Kerrian Fuller[†], Luis M. Campos[†], Saeed I. Khan[†], Natalia V. Lebedeva[‡], Malcolm D. E. Forbes[‡], and Miguel A. Garcia-Garibay[†]

[†]Department of Chemistry and Biochemistry, University of California, Los Angeles, 405 Hilgard Avenue, Los Angeles, California 90095-1569

[‡]Department of Chemistry, The University of North Carolina, Chapel Hill, North Carolina 27599-3290

Abstract

The solution photochemistry of bis(phenylpyrrolidinonyl)ketones (*R,R*)-**1b** and (*S,S*)-**1b** exhibited a remarkably high memory of chirality. Stereospecific decarbonylation to products (*R,R*)-**3b** and (*S,S*)-**3b**, respectively, occurred with an ee of ca. 80%. The reaction is thought to occur along the single state manifold by sequential Norrish type-I α -cleavage decarbonylation, and radical–radical combination in a time scale that is comparable to that required for the radical intermediate to expose its other enantiotopic face by rotation about an axis perpendicular to that of the p orbital (ca. 3–7 ps). The absolute configuration of a key intermediate and that of ketone (*R,R*)-**1b** were determined by single-crystal X-ray diffraction and the ee values of the photochemical products with the help of chiral shift reagent (+)-Eu(tfc)₃ and chiral LC-MS/MS. On the basis of the ee and de values at 25 °C, it could be determined that ca. 70% of the bond forming events occur with double memory of chirality, ca. 21% occur after rotation of one radical to form the meso product (*R,S*)-**3b**, and only 9% occur after double rotation to form the opposite enantiomer. This report represents the first example of a doubly enantiospecific Norrish type-I and decarbonylation reaction in solution and illustrates potentially efficient ways to obtain compounds with adjacent stereogenic quaternary centers.

Introduction

Reactions that display memory of chirality (MOC) were first observed by Seebach in 1981¹ but a formal definition was suggested by Fuji only about 10 years later.² MOC reactions occur enantiospecifically from reactants with sp³-hybridized chiral carbons through configurationally labile intermediates, such as carbanions, radicals, or cations,³ in the

© 2009 American Chemical Society

Correspondence to: Miguel A. Garcia-Garibay.

Supporting Information Available: Experimental data, cif files of acid **5** and ketone (*R,R*)-**1b**, spectroscopic NMR and ¹H NMR data for all new compounds, and computational details. This material is available free of charge via the Internet at <http://pubs.acs.org>.

absence of externally resolved chiral influences.⁴ MOC reactions defy the normal consequences of compromising the integrity of a chiral center by preserving its stereochemical information in the form of relatively long lived chiral conformations, which selectively expose one of the enantiotopic faces of the reactive intermediate to the incoming reagents.⁵ The structural attributes involved in MOC reactions vary widely.⁴ They include examples where the central chirality of the reactant is transiently stored in the form of axial^{2,6} or planar⁷ chirality, and cyclic structures with large inversion barriers.⁸⁻¹⁰

In the course of studying C–C bond-forming reactions by the photoinduced decarbonylation of hexasubstituted ketones, we became interested in exploring the scope and potential of their unique double memory of chirality (²MOC). While it is clear that the stepwise two-bond cleavage reactions compromise the stereochemical integrity of the two stereogenic centers (Scheme 1), we have shown that highly efficient ²MOC can be observed when the corresponding radical pairs are generated within crystalline ketones.^{11,12} Since large-amplitude molecular motions are energetically disfavored, reactions in the solid state are faster than radical rotation and the chiral information of the two stereocenters is maintained in the relative orientation of the enantiotopic faces of the two radicals.¹³ An intriguing alternative that would make it possible for ²MOC reactions to occur efficiently in fluid solvents would necessitate reactants with time scales for decarbonylation and bond formation that are faster than the time it takes for the two radicals to rotate within the solvent cage. Knowing that the time constants for rotation of medium size molecules in fluid solvents (e.g., benzene) fall in the 5–20 ps range,¹⁴ one may expect that competent ²MOC photochemical reactions will occur from the singlet excited state with reactants that have essentially no barrier for each of the two bond-cleavage steps, and which also have a spin-allowed bond forming reaction.¹⁵ While it would appear that finding reactants capable of satisfying these conditions should be very unlikely, there are a few notable examples of radical pair reactions that occur with a significant MOC at one chiral center in solution, such as the photo Arbusov reaction of optically enriched arylmethyl phosphites¹⁶ and arylmethyl phosphordiamidites,¹⁷ and the photodecarboxylation of optically enriched esters from (+)- or (–)-2-methylbutyric acid and 2,4,6-trimethylphenol.¹⁸ In this paper, we are pleased to report our results on *bis*-(*N*-methyl-phenylpyrrolidinonyl)-ketones (*R,S*)-**1b**, (*RR*)-**1b**, and (*S,S*)-**1b** (Scheme 2), which undergo a photodecarbonylation reaction with double memory of chirality through radical intermediates formed at the two α-carbons.

Our initial observations were carried out with diastereomerically pure samples of the *N*-*para*-methoxybenzyl analogue *dl*-**1a** and *meso*-**1a**, which were obtained by the stepwise coupling of 2 equiv of the 3-phenyl-pyrrolidinone anion **2**-Li with a suitable carbonyl equivalent (Scheme 2, paths *i* and *ii*).¹⁹ As described in a previous communication, we were surprised to discover that the photochemical reaction of *meso*-**1a** and *dl*-**1a** in dilute benzene solutions yielded the decarbonylation products *meso*-**3a** and *dl*-**3a** in a highly diastereospecific manner (path *iii*).¹⁹ The diastereomeric selectivity in the case of *meso*-**1a** was 2:1 in favor of *meso*-**3a**, and it changed to 1.0:2.4 in favor of *dl*-**3a** when the reaction was carried out with *dl*-**1a**. After showing that free radicals obtained by oxidation of the Li enolate of **2a** or by triplet sensitized irradiations have a 10:3 preference toward the *dl*-diastereomer (path *iv*),¹⁹ we concluded that the stereochemical information of the reactants

must be preserved by the radical pairs and relayed into the final product. Recognizing that this observation constitutes an unprecedented example of ^2MOC , we set out to confirm those results by determining the enantiospecificity of the reaction with samples of the optically pure N-methyl analogue **1b**.

We selected N-methyl derivative **1b** after showing that combination of N-methyl-3-phenylpyrrolidinone-3-yl free radicals **2'** obtained by oxidation of the carbanion **2-Li** with CuBr_2 have no diastereomeric preferences for either *dl*-**3** or *meso*-**3**. Independent photochemical experiments with dilute benzene solutions of *meso*-**1b** and *dl*-**1b** confirmed that these reactions are also diastereospecific, giving their corresponding diastereomers in a 65:35 ratio. Subsequent experiments carried out with optically pure (*R,R*)-(-)-**1b** and (*S,S*)-(+)-**1b** showed that product formation in benzene at 25 °C occurs with a significant ^2MOC . Detailed product analyses showed that 55–70% of the reactions occur with double retention, 21–35% by epimerization of a single radical center (single MOC), with only 9–12% undergoing racemization. These results confirm that the threestep reaction must occur within the time scale needed for a radical in the pair to expose its other enantiotopic face, which is estimated to be ca. 10 ps using the Stokes–Debye–Einstein model.¹⁴ This observation was confirmed also by studying the effect of temperature on the viscosity of the solvent and the enantiospecificity of the reaction, and by the lack of timeresolved chemically induced dynamic nuclear and electron polarization (CIDNP).²⁰ A negative result in this case is consistent with a radical pair that has no time to escape from the solvent cage and no spin-sorting mechanism.

Results and Discussion

Synthesis and Characterization

Diastereomerically pure samples of *dl*-**1b** and *meso*-**1b** were obtained as described previously by reaction of the lithium enolate of N-methyl-phenylpyrrolidinone **2b** with phosgene or carbonyl diimidazole (CDI) (Scheme 2).¹⁹ It should be noted that attempts to replace phosgene with a less toxic carbonyl source were met with limited success. Trichloromethyl chloroformate was effective in producing the same diastereomer *d,l* as phosgene but the product was obtained in lower yields.

The pure enantiomers of **1b** were prepared from the racemic acid (\pm)-**6** by taking advantage of a classic resolution with (*R*)-(+)- α -methyl-2-naphthalene-methanol, (*R*)-(+)- α -MNM (Scheme 3).²¹ The diastereomeric esters (+)-**4** and (-)-**5** were separated by fractional crystallization and their absolute configurations assigned with the help of an X-ray structure of crystals of diastereomer **5** obtained from ethyl acetate/hexane, which was solved in chiral space group $P2_12_12_1$. On the basis of the known configuration of (*R*)-(+)- α -MNM, we could unambiguously assign the (*R,R*) configuration to the naphthyl derivative (-)-**5** (Figure 2a).²² Hydrogenolyses²³ of the separate diastereomers gave the corresponding free acids (*S*)-(+)-**6** and (*R*)-(-)-**6** in quantitative yields. Optical rotations with nearly identical values and opposite signs were confirmed along with the expected mirror image relation in their circular dichroism (CD) spectra (Figure 1). The transformation of (*S*)-(+)-**6** and (*R*)-(-)-**6** into their corresponding acyl chlorides and subsequent reaction with the lithium enolate **2b**-

Li gave the desired ketones (*S,S*)-**1b** and (*R,R*)-**1b** in a completely diastereoselective manner. Their optical rotation and CD spectra showed signals of essentially identical magnitudes but opposite signs (Scheme 3 and Figure 1). The structure of (*R,R*)-**1b** was corroborated by X-ray diffraction with single crystals solved in the space group $P4_12_12$ (Figure 2b).²⁴

Diastereospecificity of the Photochemical Reaction of Ketones *meso*-**1b** and *dl*-**1b** in Benzene at 25 °C

As a starting point for this study, we set out to determine the intrinsic selectivity of the corresponding free radicals **2b**[•] and to confirm that the diastereospecificity of the photodecarbonylation of ketones **1b** in order to determine the suitability of the *N*-methyl protecting group. The intrinsic reactivity of free radicals **2b**[•] was established by oxidation of enolate **2b-Li** with CuBr₂ at -78 °C followed by further reaction at ambient temperature over ca. 2 h. Isolation of the products indicated no diastereomeric preference for either diastereomer, giving equimolar amounts of compounds *dl*-**3b** and *meso*-**3b**. This result can be compared with the one obtained from *N*-*para*-methoxybenzyl-protected **2a**[•], which displayed a 10:3 preference for the *meso* compound. In addition to showing no diastereomeric bias in the radical coupling process, the less-bulky *N*-methyl substituent is also an ideal probe for ¹H NMR analysis.

Photolysis experiments were carried out on 2 mM deoxygenated benzene solutions of *meso*- and *dl*-**1b** with a medium-pressure Hg Hanovia lamp with a Pyrex filter ($\lambda > 290$ nm). As observed previously, the methylene, methyl, and phenyl aromatic hydrogens of the *meso*- and *dl*-diastereomers are easily differentiated on the 500 MHz ¹H NMR spectra, allowing us to use integration to estimate the diastereomeric ratios. For example, the two equivalent *N*-methyl groups of *dl*-**3a** and *meso*-**3a** give singlets at 2.82 and 2.54 ppm, respectively. Satisfyingly, integration of the corresponding signals revealed that photolysis occurred with an appreciable diastereospecificity, giving ratios of 0.68:0.32 and 0.37:0.63 for *meso*-**3b** and *dl*-**3b**, respectively. The isolated yields of **3** were in the 40–50% range with the rest corresponding to amide **2b** (20–30%) and a few unidentified products.

Enantiospecificity of the Photochemical Reaction in Benzene at 25 °C

Irradiation experiments with the enantiopure samples (*S,S*)-**1b** and (*R,R*)-**1b** were carried out in a similar manner and the product composition analyzed by a combination of ¹H NMR, chiral LC-MS/MS, and CD spectroscopy. The diastereoselectivity of the two reactions determined by ¹H NMR analysis of the crude reaction mixture was consistent with that obtained with the racemic mixture. The integration for the *dl* and *meso*-diastereomers revealed a 65:35 ratio in favor of the chiral compound. Further analyses by ¹H NMR and CD were carried out after chromatographic separation of the two diastereomeric fractions. All analyses by chiral LC-MS/MS were carried out with the crude reaction mixture.

A rapid but qualitative assessment of the ²MOC of the photodecarbonylation reaction was established by CD measurements (Figure 3a). The samples obtained by photodecarbonylation of (*R,R*)-**3b** and (*S,S*)-**3b** gave strong and opposite CD signals with relatively sharp vibrational features that extend from ca. 250 to 290 nm (Figure 3A). It is

interesting to note that CD spectra of (*R,R*)-**3b** and (*S,S*)-**3b** are highly reminiscent of the spectra determined for the carboxylic acids (*R*)-**6** and (*S*)-**6** and quite different from the one of the corresponding ketones shown in Figure 1. The relatively high resemblance between **3b** and **6** is consistent with their common substituted benzene and lactam chromophore.

The ee of the chiral product samples was first established by measuring the ratios of the signal corresponding to the N-methyl singlet, which was well resolved upon addition of the chiral shift reagent (CSR) (+)-Eu(tfc)₃ in CDCl₃.²⁵ The results of measurements with the CSR are illustrated in Figure 3B-D with changes that occurred to the N-methyl signal. The spectra shown in Figure 3B and C correspond to the racemic sample *dl*-**3b** before and after addition of the CSR. A singlet at 2.87 ppm in Figure 3B is resolved into two equally intense singlets at ca. 2.88 and 2.81 ppm (Figure 3C), as expected for an efficient diastereomeric interaction between the bis-lactone enantiomers and the lanthanide center. The spectra shown in Figure 2D and E, measured with the samples obtained upon photolysis of (*S,S*)-**1b** and (*R,R*)-**1b**, respectively, indicate that signals at 2.88 and 2.81 ppm correspond to the decarbonylated products (*S,S*)-**3b** and (*R,R*)-**3b**, respectively. Naturally, this assignment assumes that the reaction occurs with retention and not with double inversion.

In addition to the good separation, the most striking feature of the spectra in Figure 3D and E is the relatively highly enriched enantiomeric composition of the isolated products. While integration of the ¹H NMR signals carries a ca. ±10% uncertainty,²⁶ the corresponding ee values determined for the reaction of enantiopure (*S,S*)-**1b** and (*R,R*)-**1b** were ca. 70% ± 10%. Reactions carried out to low conversion helped establish that the starting material does not epimerize under the reaction conditions, indicating that enantiomeric losses in the product do not occur by recombination of **RP1(b)** (Scheme 4). We also established with control experiments that the products are stable under the reaction conditions and that the ee does not change as a function of conversion.

In order to eliminate potential isolation artifacts and aiming to confirm and improve the accuracy of our measurements, we decided to develop an analytical protocol based on the use of chiral LC-MS/MS. Chiral LC-MS/MS also provides several advantages over chiral HPLC-UV detection. In addition to the high sensitivity, which allows us to work with small quantities of the starting material, MS/MS detection is much more specific than conventional UV detection, which does not distinguish different structures with the same chromophore. We were able to specifically detect the ketone **1b** and the photoproduct **3b** by their parent–daughter ionization transitions at 377.1/175.1 and 349.2/175.1, respectively, in a multiple reaction monitoring (MRM) mode. This method allowed us to analyze reaction mixtures with high certainty and without purification. Additionally, we were able to achieve great chiral separation using Chiralpak 1B column (Figure 4). Peaks corresponding to the *meso*-**3b**, (*R,R*)-**3b**, and (*S,S*)-**3b** displayed retention times of 6.5, 7.8, and 13.6 s with line widths of ca. 0.3–0.5 s, leaving no ambiguity in the integration.

Once the LC-MS/MS method had been optimized, we confirmed the observations previously determined by ¹H NMR (Table 1). Solution photolysis of (*S,S*)-**1b** favored the formation of (*S,S*)-**3b** (70% ± 7%) with smaller amounts of epimerization (21% ± 2%) and

double inversion products ($9\% \pm 1\%$). These results indicate a very efficient retention of chirality and a very significant ^2MOC .

Double Memory of Chirality

On the basis of the information described above and the suggested reaction mechanism,¹¹ the likely sequence of events in the ^2MOC reaction are illustrated in Scheme 4 with $(S,S)\text{-1}$. The relevant coordinates are the time scale for the bond-breaking and bond-making steps, depicted on the horizontal, and the time scale for rotation of the radicals about an axis perpendicular to the radical p orbital, shown on the vertical axis. While bond cleavage and formation involving the same face of the prochiral radical results in retention of configuration, rotation about an axis perpendicular to the axis of the radical p orbital exposes its enantiotopic face, leading to racemization of that center. It should be noted that bond dissociation at an α -carbon with the *S* or *R* configuration correlates, respectively, with formation of a radical center that exposes its prochiral *re* or *si* face with respect to the direction of the radical formed at the other α -carbon. As illustrated with structures shown in blue in the top row of Scheme 4, double memory of chirality requires that **RP1(a)**, formed by the Norrish type-I α -cleavage reaction, undergoes decarbonylation to **RP2(a)** and radical-radical combination to $(S,S)\text{-3b}$ with no radical rotation within the solvent-cage. The rotation of a single radical leads to the epimer meso $(R,S)\text{-3}$ through solvent-caged radical pairs **RP1(b)** and/or **RP2(b)**. Rotation of the two radicals leads to the enantiomer $(R,R)\text{-3b}$, which inverts the two stereocenters of the starting material. Thus, the retention of configuration in the case of **1a** (^2MOC) suggests that cleavage of the ketone α -bond, decarbonylation, and combination of the radical pair should occur within a time scale that competes with rotation of the radical fragments in benzene at 25 °C. Naturally, this hypothesis is based on the reasonable assumption that there are no strong interactions that extend the lifetime of the radical pair.

To analyze the kinetic requirements of the ^2MOC reaction, we assume that rates of bond formation (k_{comb}) for singlet radical pairs are rate and product-formation limiting. In fact, the quantum yield of reaction for ketone *dl*-**1a** is only $\Phi_{\text{R}} = 0.05$,¹⁹ indicating that **RP1(a)** goes back to the starting material ca. 95% of the times. The fact that no ketone epimerization is observed indicates that the rate of radical rotation is slower than the rate of decarbonylation, $k_{\text{rot}} < k_{\text{CO}}$. This statement is based on the fact that transitions from **RP1(a)** to **RP2(b)** would be recorded by formation $(R,S)\text{-1b}$. If we assume that radical pairs combine with a similar rate, k_{comb} , and that all radicals rotate with a rate k_{rot} , the following ordering is consistent with our experimental results: $k_{\text{comb}} \gg k_{\text{CO}} > k_{\text{rot}}$. With this assumption, the relative efficiency of the ^2MOC reaction is approximated by

$$^2\text{MOC} \approx k_{\text{CO}} / (k_{\text{CO}} + 2k_{\text{rot}}) = 0.7 \quad (1)$$

which is essentially the fraction of **RP1** undergoing decarbonylation and bond formation as compared to those where (at least) one of the two radicals rotates. The value 0.7 is taken from the yield of double retention (^2MOC product) determined by chiral LC-MS/MS in Table 1, which indicates that k_{CO} is about 4.6 times faster than k_{rot} . This simple model accounts for the amount of epimerization by single rotation (EPI) and the amount of double

rotation (INV) if one assumes that radical rotations occur prior to decarbonylation, and that multiple rotations are negligible. As the fraction of radical undergoing rotation (ROT) is the complement of those undergoing reaction (eq 2), one can formulate the yields of epimerization (EPI) and inversion (INV) as shown in eqs 3 and 4.

$$ROT \approx 1 - [k_{-CO}/(k_{-CO} + 2k_{rot})] = 0.3 \quad (2)$$

$$EPI \approx ROT(0.7) = 0.21 \quad (3)$$

$$INV \approx ROT^2(0.7) = 0.063 \quad (4)$$

Experimental values of 70%, 21%, and 9% for ²MOC, EPI, and INV in Table 1 agree remarkably well with this single passage model, suggesting that multiple radical rotations and fractionation are relatively unimportant, as expected for a very fast bond forming process.

Enantiospecificity of the Photochemical Reaction as a Function of Temperature

The time constants for rotation ($1/k_{rot}$) of the phenylpyrrolidinone radical **2**[•] about its long molecular axis in dilute benzene solutions at 298 K can be estimated as $\tau_{rot} = 6.5$ ps using the Stokes–Debye–Einstein model ($\tau_R = 4\pi\eta ab^2 fC/3k_B T$).¹⁴ To obtain this value, we assumed the molecular half axes as, $a = 4$ Å and $b = 3$ Å, the viscosity of benzene at 25 °C as $\eta = 0.60$ cP, and we used the factors $fC = 0.3$ to account for the prolate shape of the radical and a hydrodynamic slip boundary condition,²⁷ which is known to provide a good description for the hydrodynamic properties of small molecules in simple fluids.²⁸ We note that a value of $\tau_{rot} = 6.5$ ps compares very well with the ca. 7 ps experimentally obtained in benzene solutions for biphenyl, a compound that has a very similar size.²⁹ In order to test the mechanism in Scheme 4, we decided to explore the dependence of the ²MOC, EPI, and INV efficiencies with the viscosity of the solvent by doing experiments in benzene as a function of temperature. The results are summarized in Figure 5 with a plot of the product fraction as a function of temperature between 25 and 69 °C. Also shown in the figure is a line indicating the reported changes in viscosity of benzene, from 0.60 cP at 25 °C to 0.33 cP at 70 °C.³⁰ Using the latter value, the time constant for radical rotation can be calculated to decrease by a factor of 2 within this temperature range, i.e., $\tau_{rot} = 3.2$ ps at 69 °C. As can be seen in the figure, there is an excellent correlation between the ²MOC efficiency (solid red line) and the viscosity of the solvent (dotted blue line). The product fraction of (*S,S*)-**3b** decreases from 0.7 at 25 °C to 0.5 at 69 °C. This variation is accompanied by an increase in the yield of the EPI product (*S,R*)-**3b** from 21% to 35% and an increase in the INV product (*R,R*)-**3b** from 9% to 15% within the same temperature range. It is important to point out that the yield of single rotation (EPI) is always greater than the yield double rotation (INV), and that changes in the yield of single rotation occur at a faster rate than those for double rotation. These observations relate to the fact that single and double rotations are consecutive processes. Assuming the model of eq 1-4, one can see that a single passage model can no longer account for the experimental observations at the higher temperature

because multiple rotation events within the lifetime of RP1 will require a fractionation model to account for variations in the yields of the isomers.

Computational Analysis of the Effects of Substituents of the Photodecarbonylation Reaction

Knowing that the rates of α -cleavage and decarbonylation correlate with the stability of the intermediate radicals,^{11,31} it was of interest to determine whether the calculated effects of the phenyl and lactam groups would be consistent with reaction rates that take place in the picosecond regime. Starting with the structural parameters obtained from the crystal structure of ketone (*R,R*)-**1b** (Figure 2b), density functional theory (DFT) calculations were carried out to optimize key stationary points along the reaction coordinate after α -cleavage, decarbonylation, and radical–radical recombination. Enthalpies calculated by the (U)B3LYP/6-31G* method, indicate that formation of RP-1 is exothermic by 33 kcal/mol with respect to the spectroscopic singlet, and that subsequent formation of RP-2 is exothermic by 13.7 kcal/mol (Figure 6).³² Moreover, the calculated activation energy for the loss of CO from RP-1 is only 0.3 kcal/mol, which is consistent with a reaction rate of ca. $7.1 \times 10^{11} \text{ s}^{-1}$ calculated using eq 1 with the Stokes–Debye–Einstein radical rotation times. It should be noted also that this rate constant matches well the value of the pre-exponential factor determined for analogous reactions.³³ Further evidence for an ultra fast α -cleavage, decarbonylation, and combination reactions was obtained from the lack of time-resolved chemically induced dynamic nuclear polarization (CIDNP) in the ¹H NMR spectrum with ketones (*S,S*)-**1b**, *meso*-**1b**, and *dl*-**1b**. These results are consistent with a solvent-caged radical pair that has no time for evolution of the nuclear spin system and has no spin sorting events that would form products with non-Boltzmann nuclear spin populations.^{15,20,34}

Conclusions

The results reported in this paper confirm that the photodecarbonylation of bis(3-phenyl-2-pyrrolidonyl)ketones react in fluid solution with ²MOC. A detailed analysis of the diastereospecificity and enantiospecificity of the reaction was used to calculate the fraction of radical pairs that react with ²MOC by double retention, by rotation of a single radical (EPI), and by double radical rotation (INV). When these values are analyzed in terms of the times for radical rotation calculated with the Stokes–Debye–Einstein model in benzene, one can estimate that the time constant of decarbonylation in this type of structures at 25 °C falls within time scales of a few picoseconds. A qualitative confirmation of this analysis was obtained by analysis of changes in the diastereospecificity and enantiospecificity of the reaction from a series of measurements carried out in benzene as a function of temperature. The exceedingly short lifetime of the solvent-caged radical pairs is also consistent with the lack of CIDNP signals, which requires some time for the evolution of the spin system and a spin-sorting mechanism. We believe that reactions with a double memory of chirality may constitute useful probes to investigate the dynamics of low-viscosity fluids, both in homogeneous and compartmentalized systems.^{15,35} From a synthetic perspective reactions with a double memory of chirality offer opportunities for the synthesis of compounds with adjacent stereogenic quaternary centers. However, when synthetic applications are concerned, there are greater expectations for success in analogous reactions carried out in

the highly viscous and ordered environment of the crystalline ketones.¹² Ongoing work in our group includes the incorporation of solid-state ²MOC reactions in the synthesis of natural products.

Experimental Section

(3*S*)-(R)-1-(Naphthalen-3-yl)ethyl-1-methyl-2-oxo-3-phenylpyrrolidine-3-carboxylate (**4**)

A mixture of carboxylic acid **6** (0.6 g, 2.73 mmol) in oxalyl chloride (10 mL, 2 M in methylene chloride) was stirred vigorously for a period of 14 h. The yellowish solution was then concentrated under reduced pressure, washed with methylene chloride (10 mL), concentrated, and dried under high vacuum. The yellow oil was dissolved in dry methylene chloride (40 mL) and pyridine (10 mL), turning into a brown solution and stirred for one hour followed by the slow addition of a solution of (R)-(+)-1-(2-naphthyl)ethanol (0.57 g, 3.31 mmol) in methylene chloride (5 mL) and stirred for additional 2 h. The mixture was concentrated under reduced pressure and purified through column chromatography (silica, CH₃COOC₂H₅ (80%)/hexanes (20%)), yielding a yellow oil (0.24 g, 0.64 mmol, 23%) as a pure fraction corresponding to compound **4**. An additional amount of pyrrolidinone **4** (0.15 g, 0.40 mmol, 15%) was obtained by washing away the crystalline powders obtained from diethyl ether solutions corresponding to the mixed fractions of compounds **4** and **5**. [α]_D²¹ = +97.2, CHCl₃. ¹H NMR (CDCl₃) 7.81–7.79 (m, 3H), 7.73 (s, 1H), 7.52–7.30 (m, 8H), 6.09–6.05 (q, 1H, *J* = 6.6 Hz), 3.36–3.34 (m, 1H), 3.28–3.25 (m, 1H), 2.98–2.94 (m, 1H), 2.93 (s, 3H), 2.46–2.40 (m, 1H), 1.57–1.56 ppm (d, 3H, *J* = 6.6 Hz); ¹³C NMR (CDCl₃) 170.7, 169.9, 138.7, 138.0, 133.0, 132.8, 128.3, 128.1, 128.0, 127.5, 127.4, 127.3, 126.0, 125.9, 124.6, 123.7, 74.0, 60.2, 46.2, 31.8, 30.3, 22.1 ppm. FTIR (neat) 1733, 1692, 1242 cm⁻¹; HRMS (MALDI-TOF) *m/z* calcd for C₂₄H₂₃NO₃ + Na 396.1576, found 396.0014.

(3*R*)-(R)-1-(Naphthalen-3-yl)ethyl-1-methyl-2-oxo-3-phenylpyrrolidine-3-carboxylate (**5**)

The same procedure as described above for **4** was followed for **5**. [α]_D²¹ = -74.7, CHCl₃. ¹H NMR (CDCl₃) 7.76–7.71 (m, 3H), 7.54 (s, 1H), 7.46–7.31 (m, 7H), 7.25–7.24 (m, 1H), 6.07–6.03 (q, 1H, *J* = 6.6 Hz), 3.44–3.41 (m, 1H), 3.28–3.26 (m, 1H), 3.03–2.96 (m, 1H), 2.96 (s, 3H), 2.39–2.34 (m, 1H), 1.59–1.57 ppm (d, 3H, *J* = 6.6 Hz); ¹³C NMR (CDCl₃) 170.4, 170.0, 138.6, 138.3, 133.0, 132.8, 128.3, 128.0, 127.9, 127.5, 127.3, 127.2, 126.0, 125.8, 124.5, 123.8, 74.0, 60.3, 46.2, 31.9, 30.4, 22.2 ppm. FTIR (neat) 1726, 1686, 1237 cm⁻¹; HRMS (MALDI-TOF) *m/z* calcd for C₂₄H₂₃NO₃ + Na 396.1576, found 396.0021.

dl-1,1-Di-{3-[1-(4-methyl)-3-phenylpyrrolidin-2-one]yl}methanone (**dl-1b**)

To a cooled solution of (-78 °C) Me-protected pyrrolidinone **2** (0.277 g, 1.58 mmol) in tetrahydrofuran (50 mL), lithium bis(trimethylsilyl)amide (1.7 mL, 1M) was added at once and the reaction stirred for 45 min. Phosgene (0.4 mL, 20 mol % soln) was added over ~5 min, and the reaction mixture was left stirring upon warming up to -5 °C. The reaction was then quenched with a saturated ammonium chloride solution and the organic components were extracted with ether (3 × 40 mL). The combined extracts were washed with saturated aqueous sodium chloride (60 mL). The solution was then dried over MgSO₄, concentrated under reduced pressure, and purified by column chromatography (silica, CH₃COOC₂H₅

(50%)/CH₂Cl₂ (50%)) resulted in a white crystalline powder of *dl*-**1b** (0.150 g, 0.39 mmol, 50%), mp = 133–135 °C. ¹H NMR (CDCl₃) 7.34–7.31 (m, 2H), 7.28–7.25 (m, 1H), 7.24–7.21 (m, 2H), 3.34–3.27 (m, 2H), 3.1–3.05 (m, 1H), 2.87 (s, 3H), 1.92–1.87 (m, 1H), 1.92–1.87 ppm (m, 1H). ¹³C NMR (CDCl₃) 200.7, 171, 138.8, 128.6, 127.2, 127.1, 67.6, 46.4, 32.9, 30.4 ppm. FTIR (neat) 1685, 1491, 1399, 1272 cm⁻¹; HRMS (MALDI-TOF) *m/z* calcd for C₂₃H₂₄N₂O₃ + H 377.1865, found 377.1449.

meso-1,1,Di-{3-[1-(4-methyl)-3-phenylpyrrolidin-2-one]yl}methanone (meso-1b)

To a cooled solution of (–100 °C) Me-protected pyrrolidinone **2** (0.135 g, 0.77 mmol) in tetrahydrofuran (20 mL), lithium bis(trimethylsilyl)amide (1 mL, 1M) was added at once and the reaction stirred for 20 min. Carbonyl Diimidazole (CDI) (0.062 g, 0.38 mmol) was added at once and the reaction mixture was left stirring with constant warming and cooling from –115 to –75 °C over 4 h. The reaction was then quenched with a saturated ammonium chloride solution and the organic components were extracted with ether (3 × 10 mL). The combined extracts were washed with saturated aqueous sodium chloride (20 mL). The solution was then dried over MgSO₄, concentrated under reduced pressure and purified by column chromatography (silica, CH₃COOC₂H₅ (70%)/Hexanes (30%)) resulted in a white crystalline powder of *meso*-**1b** (0.050 g, 0.13 mmol, 35%), mp = 195–197 °C. ¹H NMR (CDCl₃) 7.48–7.46 (m, 2H), 7.35–7.32 (m, 2H), 7.26–7.22 (m, 1H), 3.31–3.26 (m, 1H), 2.99–2.96 (m, 1H), 2.76–2.71 (m, 1H), 2.56 (s, 3H), 2.33–2.27 ppm (m, 1H). ¹³C NMR (CDCl₃) 201.5, 170.3, 138, 128.2, 127.5, 127.4, 66.5, 45.6, 31.2, 29.9 ppm. FTIR (neat) 1712, 1677, 1495, 1271 cm⁻¹; HRMS (MALDI-TOF) *m/z* calcd for C₂₃H₂₄N₂O₃ + Na 399.1685, found 398.9608.

(S)-1-Methyl-2-oxo-3-phenylpyrrolidine-3-carboxylic acid [(S)-6b]

H₂ gas was bubbled into a solution of Naphthyl ester **4** (0.05 g, 0.11 mmol) in 10 mL of ethyl acetate. Palladium on carbon 10 wt % (17 mg) was added and the flask was secured applying a pressure of H₂ (ca. 15 psi) with vigorous stirring for two hours. The black suspension was filtered over a bed of Celite and the filtrate concentrated over reduced pressure. Recrystallization with ethyl ether yielded the corresponding acid (*S*)-**6** in quantitative yields (0.023 g, 0.011 mol) as colorless crystals. [α]²¹_D = + 195.2, CHCl₃. ¹H NMR (CDCl₃) 7.43–7.37 (m, 5H), 3.39–3.36 (m, 2H), 3.10 (s, 3H), 2.93–2.87(m, 1H), 2.60–2.56 ppm (m, 1H); ¹³C NMR (CDCl₃) 174.2, 170.7, 136.7, 129.1, 128.4, 126.0, 58.8, 45.9, 31.5, 30.4 ppm. FTIR (neat) 1726, 1653, 1212 cm⁻¹; HRMS (MALDITOF) *m/z* calcd for C₁₂H₁₃N₂O₃ + Na 242.0793, found 241.9872.

(S,S)-1,1,Di-{3-[1-(4-methyl)-3-phenylpyrrolidin-2-one]yl}methanone (S,S)-1b

A mixture of carboxylic acid (*S*)-**6b** (0.13 g, 0.59 mmol) in oxalyl chloride (10 mL, 2 M in methylene chloride) was stirred vigorously for a period of 14 h. The yellowish solution was then concentrated under reduced pressure, washed with methylene chloride (10 mL), concentrated, and dried under high vacuum. The yellow oil was dissolved in dry tetrahydrofuran and added to a flask containing the enolate form of **2** at –78 °C formed as follows. To a cooled (–78 °C) solution of **2** (0.105 g, 0.6 mmol) in THF (10 mL) was added lithium bis(trimethylsilyl)amide (0.65 mL, 1M) and stirred for 30 min. The mixture of the

acyl chloride of (*S*)-**6b** and the enolate of **2** was stirred until a temperature of ca. -40° was reached and then quenched with a saturated ammonium chloride solution; the organic components were extracted with ether (3×20 mL). The combined extracts were washed with saturated aqueous sodium chloride (20 mL). The solution was then dried over MgSO_4 , concentrated under reduced pressure, and purified by column chromatography (silica, $\text{CH}_3\text{COOC}_2\text{H}_5$ (80%)/hexanes (20%)) resulting in a white crystalline powder of compound (*S,S*)-**1b** (0.13 g, 0.34 mmol, 58%). $[\alpha]_D^{23} = +244.5$, CHCl_3 . $^1\text{H NMR}$ (CDCl_3) 7.34–7.22 (m, 5H), 3.34–3.30 (m, 2H), 3.08–3.07 (m, 1H), 2.88 (s, 3H), 1.93–1.90 ppm (m, 1H); $^{13}\text{C NMR}$ (CDCl_3) 200.7, 171, 138.8, 128.6, 127.2, 127.1, 67.6, 46.4, 32.9, 30.4 ppm. FTIR (neat) 1685, 1491, 1399, 1272 cm^{-1} ; HRMS (MALDI-TOF) m/z calcd for $\text{C}_{23}\text{H}_{24}\text{N}_2\text{O}_3 + \text{Na}$ 399.1685, found 398.9867.

(*R*)-1-Methyl-2-oxo-3-phenylpyrrolidine-3-carboxylic Acid [(*R*)-**6b**]

The same procedure as that described for compound (*S*)-**6b** above was followed to obtain the corresponding acid (*R*)-**6b** in quantitative yields in the form of colorless crystals. $[\alpha]_D^{21} = -194.1$, CHCl_3 . $^1\text{H NMR}$ (CDCl_3) 7.46–7.36 (m, 5H), 3.39–3.36 (m, 2H), 3.10 (s, 3H), 2.93–2.87 (m, 1H), 2.60–2.56 ppm (m, 1H); $^{13}\text{C NMR}$ (CDCl_3) 174.2, 170.7, 136.7, 129.1, 128.4, 126.0, 58.8, 45.9, 31.5, 30.4 ppm. FTIR (neat) 1726, 1654, 1211 cm^{-1} ; HRMS (MALDI-TOF) m/z calcd for $\text{C}_{12}\text{H}_{13}\text{N}_2\text{O}_3 + \text{Na}$ 242.0793, found 242.0539.

(*R,R*)-1,1-Di-{3-[1-(4-methyl)-3-phenylpyrrolidin-2-one]yl}methanone (*R,R*)-**1b**

The same procedure as that described for compound (*S,S*)-**1** above was followed to obtain the corresponding acetone (*R,R*)-**1b** in the form of white crystalline powders recording slightly higher yields (69%). $[\alpha]_D^{23} = -240.8$, CHCl_3 . $^1\text{H NMR}$ (CDCl_3) 7.35–7.22 (m, 5H), 3.36–3.28 (m, 2H), 3.11–3.06 (m, 1H), 2.88 (s, 3H), 1.93–1.88 ppm (m, 1H); $^{13}\text{C NMR}$ (CDCl_3) 200.7, 171, 138.8, 128.6, 127.2, 127.1, 67.6, 46.4, 32.9, 30.4 ppm. FTIR (neat) 1685, 1491, 1399, 1272 cm^{-1} ; HRMS (MALDI-TOF) m/z calcd for $\text{C}_{23}\text{H}_{24}\text{N}_2\text{O}_3 + \text{Na}$ 399.1685, found 398.9422.

meso-3,3-Bis(1-methyl-3-phenylpyrrolidin-2-one) (*meso*)-**3b**

To a cooled (-78°C) solution of **2** (0.19 g, 1.08 mmol) in dried and degassed tetrahydrofuran (50 mL), lithium bis(trimethylsilyl)amide (5.4 mL, 1M) was added at once and the reaction stirred for 25 min. Copper(II) bromide (1.21 g, 5.4 mmol) was added at once and the reaction mixture was left stirring while slowly warming to room temperature over a period of ca. 3 h. The reaction was then quenched with a saturated ammonium chloride solution and the organic components were extracted with ether (3×10 mL). The combined extracts were washed with saturated aqueous sodium chloride (20 mL). The solution was then dried over Na_2SO_4 , concentrated under reduced pressure, and purified by column chromatography (silica, $\text{CH}_3\text{COOC}_2\text{H}_5$). The first fraction was collected as a white crystalline powder and identified as compound *meso*-**3b** (0.035 g, 0.1 mmol, 9.2%). $^1\text{H NMR}$ (CDCl_3) 7.95–7.93 (m, 2H), 7.34–7.3 (m, 2H), 7.26–7.23 (m, 1H), 3.51–3.46 (m, 1H), 2.77–2.73 (m, 1H), 2.54 (s, 3H), 2.44–2.39 (m, 1H), 1.97–1.92 ppm (m, 1H); $^{13}\text{C NMR}$ (CDCl_3) 173.9, 140.7, 128.8, 127.5, 127.1, 56.6, 46.1, 29.8, 29.3 ppm. FTIR (neat) 1667,

1396, 1264 cm^{-1} ; HRMS (MALDI-TOF) m/z calcd for $\text{C}_{22}\text{H}_{24}\text{N}_2\text{O}_2 + \text{Na}$ 371.1735, found 370.9512.

***dl*-3,3-Bis(1-methyl-3-phenylpyrrolidin-2-one) (*dl*-3b)**

The same procedure to obtain compound *meso*-3 (above) was employed. Purification through column chromatography (silica, $\text{CH}_3\text{COOC}_2\text{H}_5$) resulted in the more polar fraction being isolated as a white crystalline powder and identified as compound *dl*-3 (0.042 g, 0.12 mmol, 11.1%). ^1H NMR (CDCl_3) 7.33–7.27 (m, 5H), 3.5–3.46 (m, 1H), 3.2–3.17 (m, 1H), 2.85 (m, 1H), 2.82 (s, 3H), 1.81–1.78 ppm (m, 1H); ^{13}C NMR (CDCl_3) 175.5, 136.9, 129.1, 127.4, 127.2, 55.5, 45.4, 30.1, 29.0 ppm. FTIR (neat) 1669, 1397, 1269 cm^{-1} ; HRMS (MALDI-TOF) m/z calcd for $\text{C}_{22}\text{H}_{24}\text{N}_2\text{O}_2 + \text{Na}$ 371.1735, found 371.1153.

Enantiomeric Excess Determination for (*R*)- or (*S*)-3,3-Bis(1-methyl-3-phenylpyrrolidin-2-one), (*R*)- or (*S*)-3

Benzene millimolar solutions (ca. 3 mM) of either (*S,S*)-1 or (*R,R*)-1 were prepared and degassed with Argon gas for 30 min. All samples were placed at similar distances (ca. 10 cm) from a medium pressure Hg Hanovia lamp ($\lambda > 290$ nm) and stirred while keeping the reaction at room temperature. The solutions were concentrated under reduced pressure and purified through column chromatography (silica, $\text{CH}_3\text{COOC}_2\text{H}_5$ (80%)/hexanes (20%)). Dissolution of the corresponding products in CDCl_3 followed by addition of 0.5 equiv of europium tris[3-(trifluoromethylhydroxymethylene)-(+)-camphorate] lead to separation of the corresponding N- CH_3 signals. Integration of these signals provided the reported ee values.

Variable-Temperature Photolysis

To perform variable-temperature experiments, a reaction setup was devised that would place the sample in contact with the vapors of an appropriate refluxing solvent in order to maintain the temperature as constant and as accurate as possible. For example, for a photolysis at 69 °C, a sealed tube with ca. 2 mM (*S,S*)-1b in deoxygenated benzene was suspended over refluxing *n*-hexane and once the reflux had equilibrated the sample was exposed to the output of the UV lamp. Additional experiments at 35, 41, and 56 °C were carried out, respectively, under vapors of refluxing diethyl ether, dichloromethane, and acetone.

Time-Resolved CIDNP Experiments

These experiments were run on a 200 MHz Bruker instrument with 308 nm excitation of 13 mM samples of compounds (*S,S*)-1b, *dl*-1b, and *meso*-1b in deuterated benzene at room temperature, with a 3 μs rf pulse. Samples were presaturated with random high-power rf pulses to eliminate dark NMR signals. Spectra were acquired at 0, 20, and 100 μs after the laser flash and showed no enhancement above Boltzmann spin state populations. A test system of dicumyl ketone was run first at a similar optical density and with the same spectrometer settings. The test system exhibited strong CIDNP signals at the same delay times after the laser flash.

Supplementary Material

Refer to Web version on PubMed Central for supplementary material.

Acknowledgments

This work was supported by NSF Grant No. CHE0551938 and National Center for Research Resources (Grant No. S10RR024605). We thank A. Dooley for help with MS.

References

1. Seebach D, Wasmuth D. *Angew Chem Int Ed.* 1981; 20:971.
2. Kawabata T, Yahiro K, Fuji K. *J Am Chem Soc.* 1991; 113:9694.
3. Matsumura Y, Shirakawa W, Satoh Y, Umino M, Tanaka T, Maki T, Onomura O. *Org Lett.* 2000; 2:1689. [PubMed: 10880202]
4. Zhao H, Hsu DC, Carlier PR. *Synthesis.* 2005; 1:1.
5. (a) Griesbeck AG, Hoffmann N, Warzecha K-D. *Acc Chem Res.* 2007; 40:128. [PubMed: 17256976] (b) Herrera AJ, Rondón M, Suárez E. *Synlett.* 2007; 12:1851.(c) Wanyoike GN, Onomura O, Maki T, Matsumura Y. *Org Lett.* 2002; 4:1875. [PubMed: 12027636] (d) Kawabata T, Chen J, Suzuki H, Nagae Y, Kinoshita T, Chancharunee S, Fuji K. *Org Lett.* 2000; 2:3883. [PubMed: 11101444] (e) Giese B, Barbosa F, Stähelin C, Sauer S, Wettstein P, Wyss C. *Pure Appl Chem.* 2000; 72:1623.
6. (a) Beagley B, Betts MJ, Pritchard RJ, Schofield A, Stoodley RJ, Vohra S. *Chem Commun.* 1991:924.(b) Beagley B, Betts MJ, Pritchard RJ, Schofield A, Stoodley RJ, Vohra S. *J Chem Soc, Perkin Trans.* 1993; 1:1761.(c) Betts MJ, Pritchard RJ, Schofield A, Stoodley RJ, Vohra S. *J Chem Soc, Perkin Trans.* 1999; 1:1067.
7. Schmalz H-G, Koning CBD, Bernicke D, Siegel S, Pfeldtschinger A. *Angew Chem, Int Ed.* 1999; 38:1620.
8. Carlier PR, Zhao H, De Guzman J, Lam PC-H. *J Am Chem Soc.* 2003; 125:11482. [PubMed: 13129335]
9. (a) Griller D, Ingold K, Krusic PJ, Fisher H. *J Am Chem Soc.* 1978; 100:6750.(b) Buckmelter AJ, Kim A, Rychmosky SD. *J Am Chem Soc.* 2000; 122:9386.
10. Sakamoto M, Kawanishi H, Mino T, Kasashima Y, Fujita T. *Chem Commun.* 2006:4608.
11. Garcia-Garibay, MA.; Campos, L. *CRC Handbook of Organic Photochemistry.* Horspool, W., editor. CRC Press; Boca Raton, FL: 2003.
12. (a) Mortko CJ, Garcia-Garibay MA. *Top Stereochem.* 2006; 25:205.(b) Natarajan A, Ng D, Yang Z, Garcia-Garibay MA. *Angew Chem Int Ed.* 2007; 46:6485.(c) Ng D, Yang Z, Garcia-Garibay MA. *Org Lett.* 2004; 6:645. [PubMed: 14961644]
13. Radical intermediates with single MOC have been documented also in other viscous media such lipid bilayers and polyethylene films. Brittain WJ, Porter NA, Krebs PJ. *J Am Chem Soc.* 1984; 106:7652.. Xu J, Weiss RG. *Org Lett.* 2003; 5:3077. [PubMed: 12916985]
14. (a) Fleming, GR. *Chemical Applications of Ultrafast Spectroscopy.* Oxford University Press; New York: 1986. (b) Buchachenko AL, Wasserman AM, Kovarskii AL. *Int J Chem Kinet.* 2004; 1:361.
15. Turro NJ, Buchachenko AL, Tarasov VF. *Acc Chem Res.* 1995; 28:61.
16. Bhanthumnavin W, Bentrude WG. *J Org Chem.* 2001; 66:980. [PubMed: 11430121]
17. Bhanthumnavin W, Bentrude WG. *J Org Chem.* 2005; 70:4643. [PubMed: 15932300]
18. Mori T, Weiss RG, Inoue Y. *J Am Chem Soc.* 2004; 126:8961. [PubMed: 15264827]
19. Resendiz MJE, Natarajan A, Garcia-Garibay MA. *Chem Commun.* 2008:193.
20. Harbron, EJ.; Forbes, MDE. *Encyclopedia of Chemical Physics and Physical Chemistry.* Vol. Chapter B1.17. Institute of Physics Publishing; London: 2001. p. 1389-1417.
21. Vávra J, Vodička P, Streinz L, Bud šínský M, Koutek B, Ondráček J, Čisářova I. *Chirality.* 2004; 16:652. [PubMed: 15455444]

22. Crystal data for **5** at 100(2) K: C₂₄H₂₃NO₃, FW 373.43, orthorhombic, space group *P*2₁2₁2₁, *a* = 9.1259(18) Å, *b* = 11.164(2) Å, *c* = 19.548(4) Å, $\alpha = 90^\circ$, $\beta = 90^\circ$, $\gamma = 90^\circ$, *V* = 1991.7(7) Å³, *Z* = 4, $\delta_{\text{calcd}} = 1.245 \text{ Mg/m}^3$, *F*(000) = 792, $\lambda = 0.71073 \text{ \AA}$, $\mu (\text{Mo K}\alpha) = 0.355 \text{ mm}^{-1}$, crystal size = 0.20 × 0.20 × 0.10 mm³; of the 2787 reflections collected, 2277 [*R*(int) = 0.0554] were independent reflections; max/min residual electron density 0.392 and -0.317 e · Å⁻³, *R*1 = 0.0554 (*I* > 2 σ (*I*)) and *wR*2 = 0.0911.
23. Theisen PD, Heathcock CH. *J Org Chem.* 1993; 58:142.
24. Crystal data for (*R, R*)-**1** at 110(2) K: C₂₃H₂₄N₂O₃, FW 376.44, tetragonal, space group *P*4₁2₁2, *a* = 6.8604(13) Å, *b* = 6.8604(13) Å, *c* = 40.242(11) Å, $\alpha = 90^\circ$, $\beta = 90^\circ$, $\gamma = 90^\circ$, *V* = 1894.0(7) Å³, *Z* = 4, $\delta_{\text{calcd}} = 1.320 \text{ Mg/m}^3$, *F*(000) = 800, $\lambda = 0.71073 \text{ \AA}$, $\mu (\text{Mo K}\alpha) = 0.355 \text{ mm}^{-1}$, crystal size = 0.30 × 0.20 × 0.10 mm³; of the 1497 reflections collected, 1398 [*R*(int) = 0.0635] were independent reflections; max/min residual electron density 0.392 and -0.317 e · Å⁻³, *R*1 = 0.0591 (*I* > 2 σ (*I*)) and *wR*2 = 0.1339.
25. (a) Kagawa M, Machida Y, Nishi H, Haginaka J. *J Pharm Biomed Anal.* 2005; 38:918. [PubMed: 16024206] (b) Sanders JKM, Williams DH. *Nature.* 1972; 240:385.
26. Pieters LA, Vlietinck AJ. *J Pharm Biomed Anal.* 1989; 7:1405. [PubMed: 2490526]
27. Hu C-M, Zwanzing R. *J Chem Phys.* 1974; 60:4354.
28. Williams AM, Jiang Y, Ben-Amotz D. *Chem Phys.* 1994; 180:119.
29. Benzler J, Luther K. *Chem Phys Lett.* 1997; 279:333.
30. Lide, DR., editor. *Values taken from CRC Handbook of Chemistry and Physics.* CRC Press; Boca Raton, FL: 2007.
31. Fisher H, Paul H. *Acc Chem Res.* 1987; 20:200.
32. This method has been previously shown to give reasonable estimates or radical stabilization energies. Please see the following and references therein: Campos LM, Ng D, Yang Z, Dang H, Martinez HL, Garcia-Garibay MA. *J Org Chem.* 2002; 67:3749. [PubMed: 12027689]
33. Gould IR, Baretz BH, Turro NJ. *J Am Chem Soc.* 1987; 91:925.
34. Sagdeev RZ, Bagryanskaya EG. *Russ Chem Rev.* 2000; 69:925.
35. Kalyanasundaram, K. *Photochemistry in Microheterogeneous Systems.* Academic Press; New York: 1987.

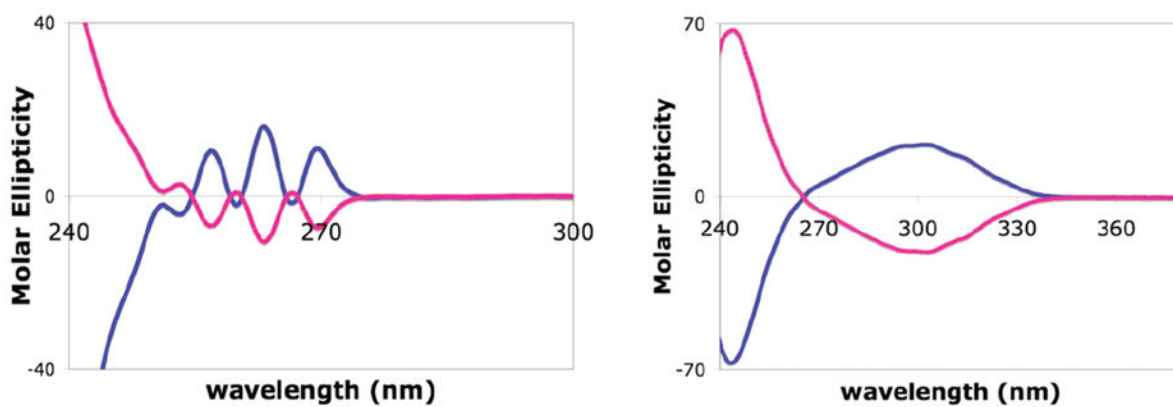


Figure 1. (Left) CD spectra of (*S*)-(+)-**6** (blue line) and (*R*)-(-)-**6** (red line). (Right) CD spectra of (*S,S*)-(+)-**1** (blue line) and (*R,R*)-(-)-**1** (red line).

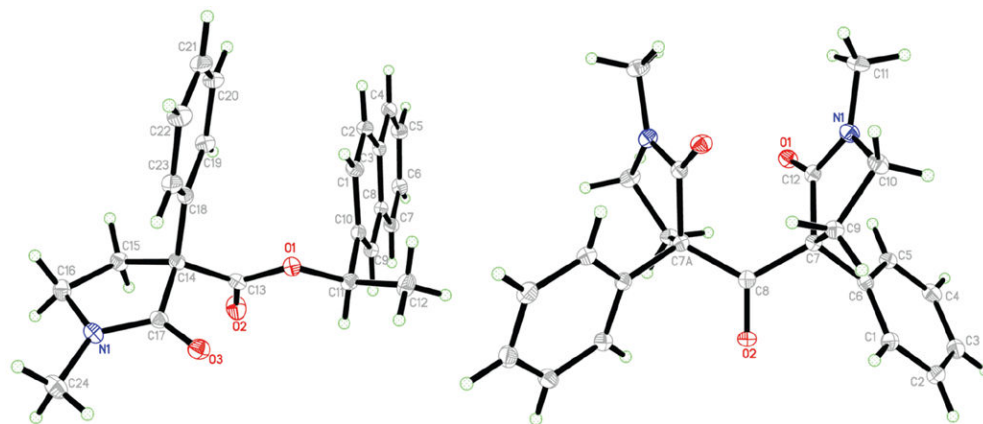


Figure 2. ORTEP diagrams of (a) (*R*)-(+)- α -methyl-2-naphthalene-methylester **5** (left) and (b) ketone (*R,R*)-**1b** (right).

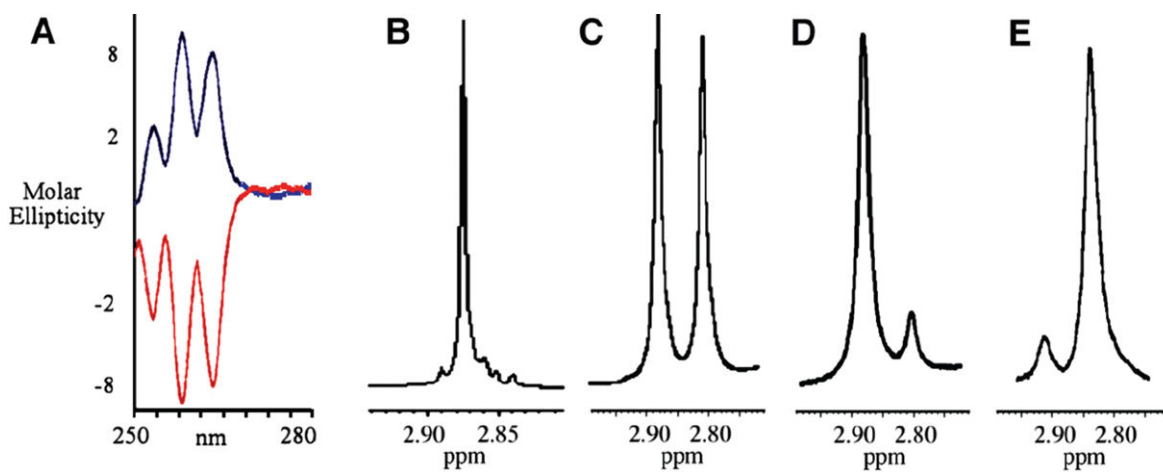


Figure 3.

(A) CD spectra from samples of (+)-(*S,S*)-**3b** and (-)-(*R,R*)-**3b**. (B) ¹H NMR signal the N-CH₃ protons in CDCl₃ of a racemic sample, (C) of a racemic sample with (+)-Eu(tfc)₃ added, (D) of a photolyzed and purified sample of (*R,R*)-**1b** with (+)-Eu(tfc)₃, and (E) of a photolyzed and purified sample of (*S,S*)-**1b** with (+)-Eu(tfc)₃ added.

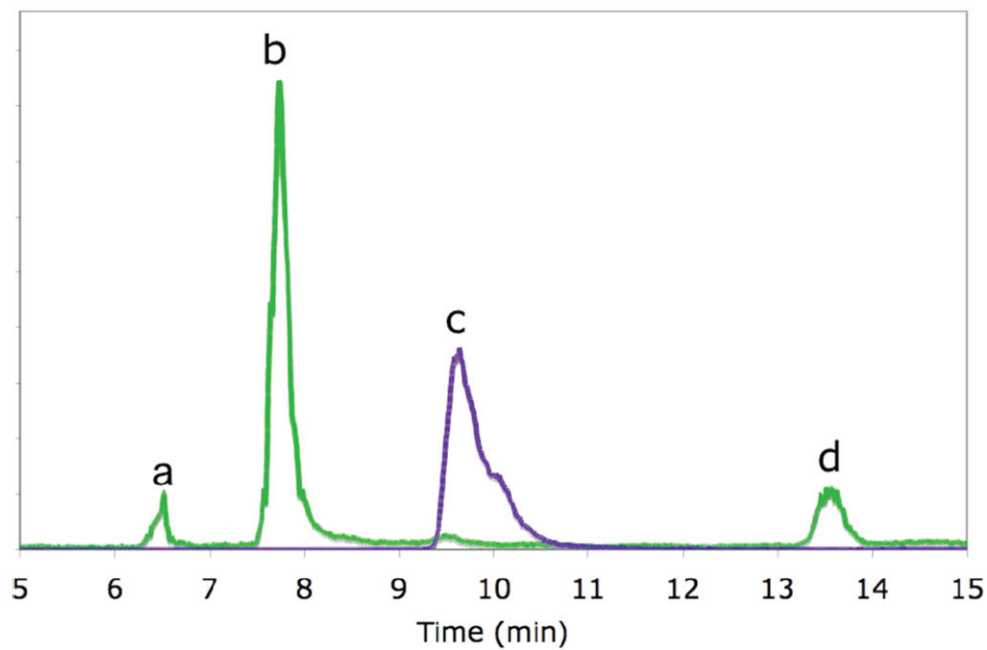


Figure 4. Chromatogram using LC-MS/MS where peak a is the *meso*-**3b**, peak b is (*S,S*)-**3b**, peak c is (*S,S*)-**1b**, and peak d is (*R,R*)-**3b**. The green trace is the 349.2/175.1 transition specific to (*S,S*)-**1b**, and the purple is the 377.1/175.1 transition specific to the isomers **3b**.

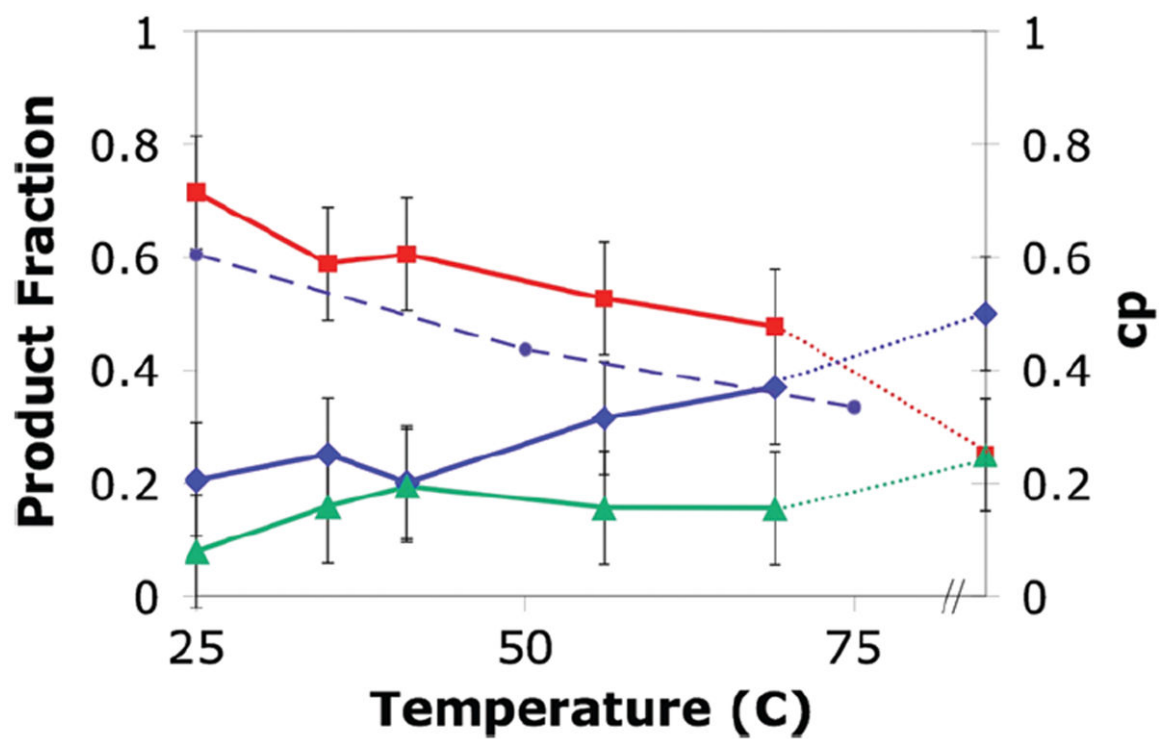


Figure 5. Product fraction of (*S,S*)-**3b** (red line with squares), *meso*-**3b** (blue line with diamonds), and (*R,R*)-**3b** (green line with triangles) as a function of temperature. The viscosity is shown as a function of temperature in the dotted line with circles. The dotted red, blue, and green lines lead to the product fractions of the free-radical reaction.

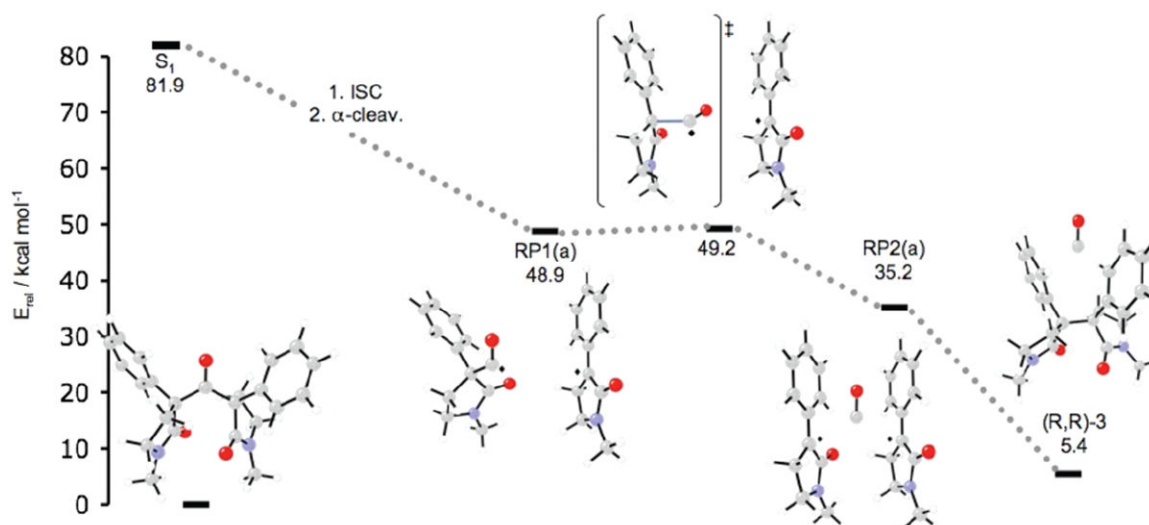
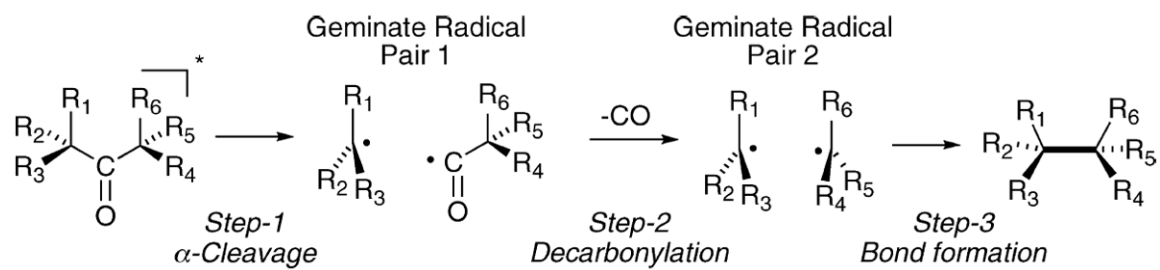
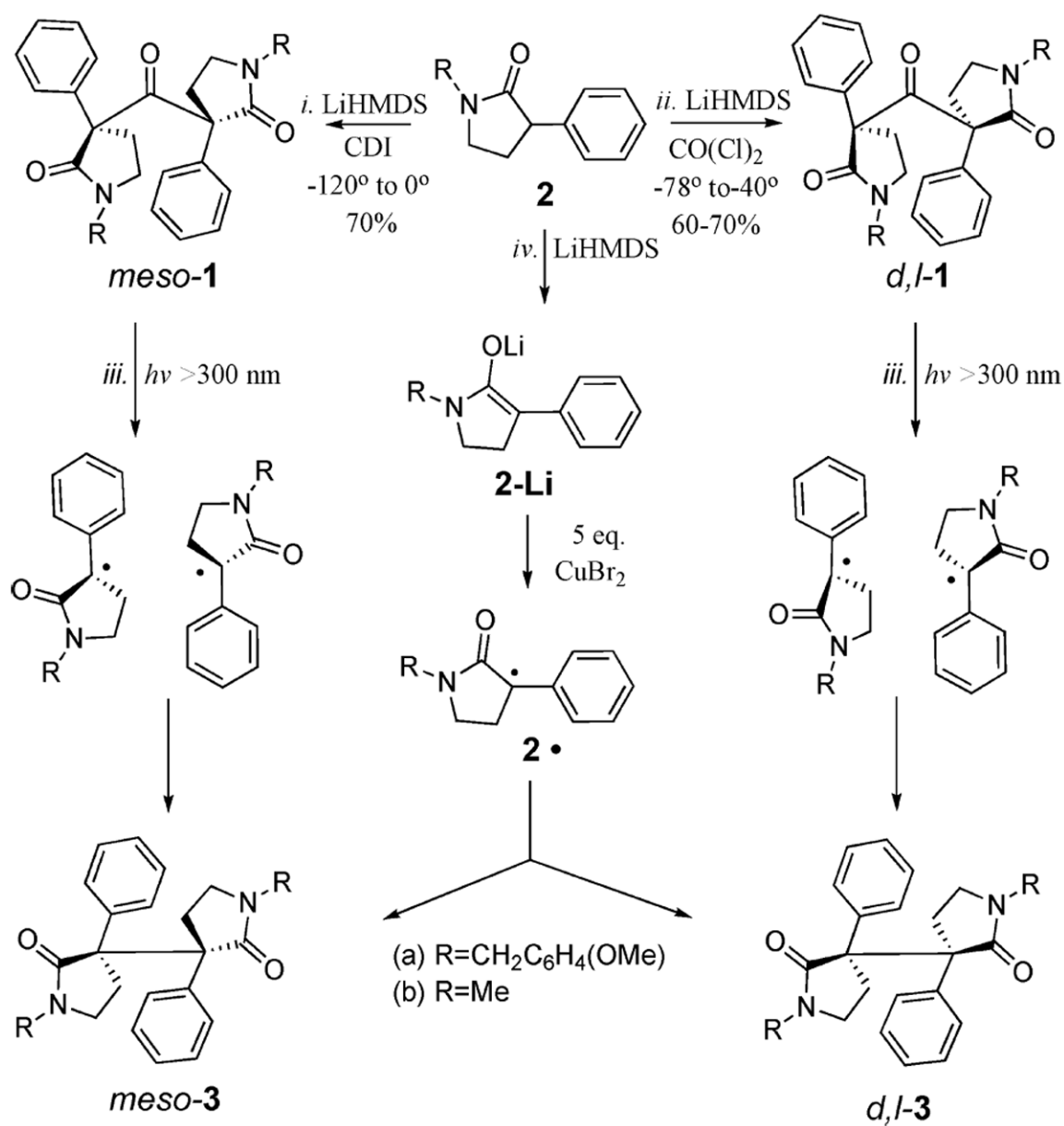


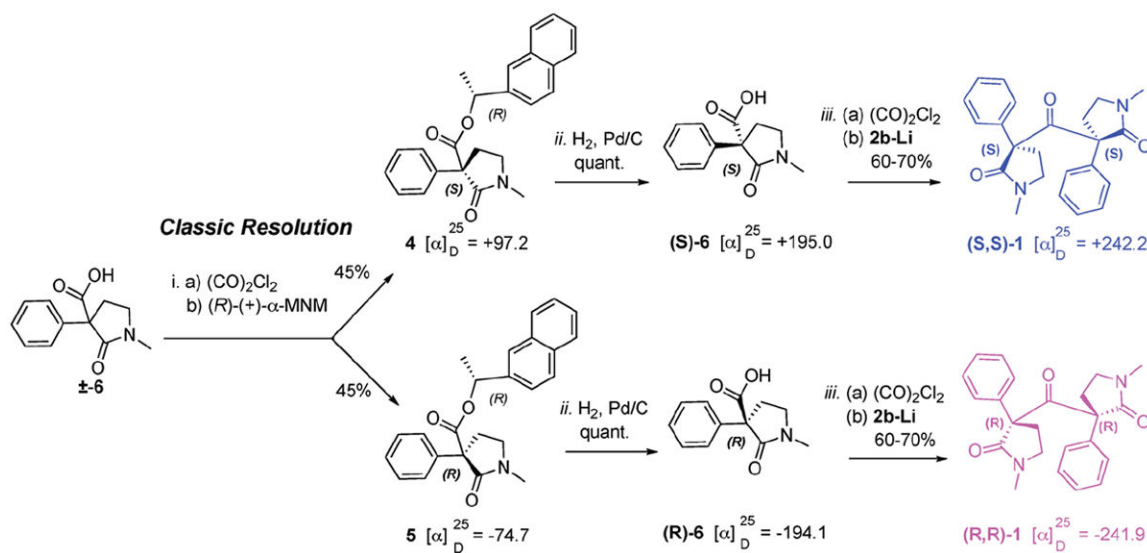
Figure 6. Structures along the reaction coordinate for the decarbonylation of ketone (*R,R*)-**1b** to yield (*R,R*)-**3b**.



Scheme 1.
Double Memory of Chirality (2 MOC)



Scheme 2.



Scheme 3.

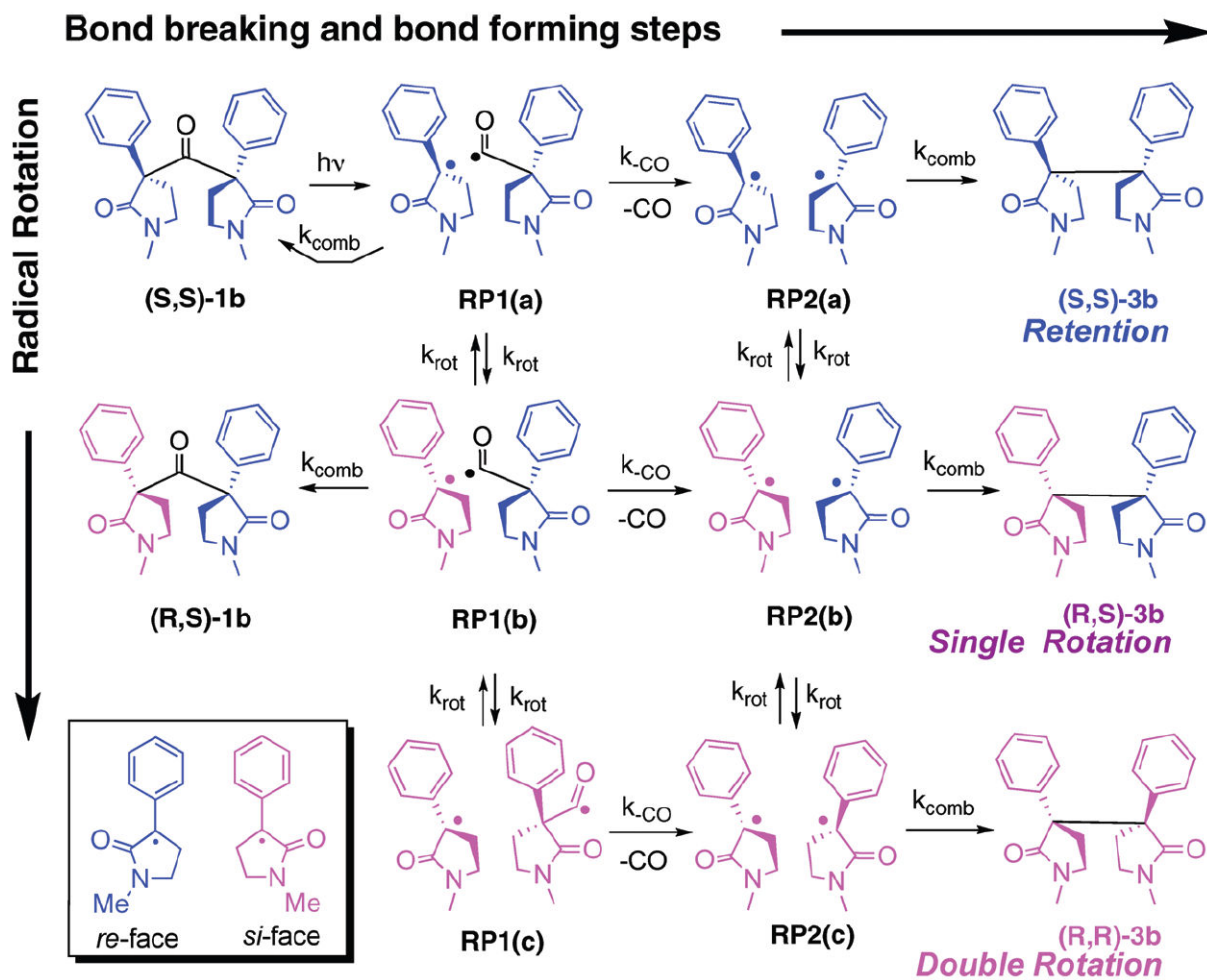


Table 1

Results from the Photolysis of Optically Pure Ketones (*S,S*)-**1b** and (*R,R*)-**1b** That Proceeded by Complete Retention (²MOC), Single Rotation (EPI), and Double Rotation (INV) As Determined by CSR and Chiral LC-MS/MS

mode of reaction	product fraction	
	based on ¹ H NMR CSR	based on LC MS/MS
retention (² MOC)	0.65 ± 0.06	0.70 ± 0.07
single rotation (EPI)	0.35 ± 0.04	0.21 ± 0.02
double rotation (INV)	0.10 ± 0.01	0.09 ± 0.01